arXiv:1302.1705v1 [gr-qc] 7 Feb 2013

Dynamics of test particles in thin-shell wormhole spacetimes

Valeria Kagramanova and Elena Smolarek
Institut für Physik, Universität Oldenburg, D–26111 Oldenburg, Germany

(Dated: February 8, 2013)

Geodesic motion in traversable Schwarzschild and Kerr thin-shell wormholes is studied. The orbits are calculated exactly in terms of elliptic functions and visualized with the help of embedding diagrams.

PACS numbers: 04.20.Jb, 02.30.Hq

I. INTRODUCTION

The idea to travel in the twinkling of an eye from one region of the Universe to another, no matter how far, or even to travel in time has been fascinating people since many years. Wormholes are believed to make such dreams possible. The first solution providing such a saught for connection between distant locations was discovered by Einstein and Rosen [1], the Einstein-Rosen bridge. Wheeler gave it the name wormhole [2]. But unfortunately this first wormhole was not traversable [3].

For Sagan's novel "Contact" Morris and Thorne devised a wormhole which could in principle be traversed by humans [4]. Visser [5, 6] provided further examples of traversable wormholes. In particular, he constructed such wormholes by surgically manipulating the Schwarzschild spacetime so that no event horizon was present. In both cases, the price to pay is the need for an exotic form of matter that must be present at the throat of such wormholes. Moreover, such wormholes should be stable if they are traversable. Visser [6] stressed that certain equations of state would lead to stable wormholes.

The material comprising the throat of the wormhole was addressed in many scientific works and is still an active field of research. For example, a phantom scalar field was discussed in [7–11], 'tachyon matter' as a source term in the field equations with a positive cosmological constant was studied in [12], or the wormhole geometry with a Chaplygin gas in the exotic equation of state was explored in [13]. An interesting discussion of a perfect fluid and an anisotropic fluid as candidates for the exotic matter was given in [14]. Estimates on the amount of exotic matter necessary for the traversability were given in [15]. A combined model comprising ordinary and quintessential matter can support a traversable wormhole in Einstein-Maxwell gravity as shown in [16]. Further references can be found in the book of Visser [17] and in the overview by Lobo [18]. The appearance of wormholes in string theory was investigated in [19, 20].

Stable spherical wormholes which do not need any form of exotic matter for their existence were recently obtained numerically in dilatonic Einstein-Gauss-Bonnet theory in four spacetime dimensions [21, 22]. Besides their stability the authors studied their domain of existence, they investigated their geodesics, determining the possible types of trajectories, and performed a study of the acceleration and tidal forces that a traveler crossing such a wormhole would feel. Further numerically obtained configurations of wormholes were explored in [23, 24], where wormholes were filled by a perfect fluid (ordinary matter) and a phantom scalar field. This model was applied to describe stars as well as neutron stars with a nontrivial topology.

A comprehensive investigation of the geodesics in the Morris-Thorne wormhole spacetime was carried out in [25], where for visualization of the trajectories embedding diagrams were constructed. Moreover, gravitational lensing and illumination calculations were addressed. Further properties of the propagation of particles and fields in static spherically symmetric wormhole spacetimes were studied in [26].

Rotating wormholes are a natural generalization of the initially studied, static spherically symmetric wormholes, that are interesting from a physical point of view. For instance, one can construct a thin-shell rotating wormhole [14] by the same cut-and-paste method [6] used for the thin-shell static wormhole. On the other hand, generalizations of the Morris-Thorne wormhole [4] were presented by Teo [27] and Kuhfittig [28]. These wormholes are traversable and due to the rotation and a possible ergoregion (for not too wide a throat) an extraction of energy by the Penrose process is possible. Slowly rotating wormholes with a phantom scalar field were studied in [29, 30]. The electromagnetic field generation around rotating wormholes surrounded by charged particles was studied in [31]. In [32] a class of rotating and magnetized wormholes with Einstein-–Maxwell and phantom fields was explored.

The conversion of a wormhole into a time machine, the problems appearing thereby and accompanying physical effects were discussed in [33–35]. The associated problems of causality violations were addressed in [36, 37].

In this article we study the motion of massive and massless particles in thin-shell Schwarzschild and Kerr wormhole spacetimes, constructed by the cut-and-paste method [6, 14]. Thus the paper contains two main sections. Section II explores the dynamics of null and timelike geodesics for static spherically symmetric thin-shell wormholes and Section III - the geodesics for rotating thin-shell wormholes. We also study the influence of the ergoregion, existing for sufficiently thin throats, on the properties of the orbits. The trajectories are given by exact analytical solutions of the geodesic equations in terms of the Jacobi and Weierstrass elliptic functions.

II. SCHWARZSCHILD WORMHOLE

We start with the geodesic equation for a test particle in the equatorial plane (see e.g. [38–40])

$$\left(\frac{dr}{d\varphi}\right)^2 = \frac{r^4}{L^2}\left(E^2 - \left(\delta + \frac{L^2}{r^2}\right)\left(1 - \frac{1}{r}\right)\right) , \qquad (1)$$

where E is the dimensionless energy of a test particle, L is its dimensionless angular momentum, $\delta = 0$ for null and $\delta = 1$ for time-like geodesics. The radial coordinate r is normalized to $2M$ and is also dimensionless.

The substitution $r = u^{-1}$ reduces (1) to the form

$$\left(\frac{du}{d\varphi}\right)^2 = u^3 - u^2 + \frac{\delta}{L^2}u + \frac{E^2-\delta}{L^2} . \qquad (2)$$

The differential (2) is elliptic of the first kind and can be integrated by Jacobi elliptic functions. To reduce it to the standard form we make two transformations. The first one $u = 4v + \frac{1}{3}$ transforms (2) into the Weierstrass form

$$\left(\frac{dv}{d\varphi}\right)^2 = 4\prod_{i=1}^{3}(v - v_i) = 4v^3 - g_2 v - g_3 , \qquad (3)$$

where $\sum_{i=1}^{3} v_i = 0$, $g_3 = 4v_1v_2v_3$ and $g_2 = 4v_3^2 - 4v_1v_2$.

The second transformation $v = (v_2 - v_1)t^{-2} + v_1$ turns (3) into

$$\frac{1}{v_2 - v_1}\left(\frac{dt}{d\varphi}\right)^2 = (1-t^2)(1-m^2t^2) , \qquad (4)$$

where $m^2 = (v_3 - v_1)(v_2 - v_1)^{-1}$, and m is the modulus of the Jacobian elliptic functions [42].

With Jacobi's elliptic function $sn(x)$ we find from (4) t as a function of φ:

$$t = sn\Big((\varphi - \varphi')\sqrt{v_2 - v_1}\Big) , \qquad (5)$$

where

$$\varphi' = \varphi_0 + \frac{1}{\sqrt{v_2 - v_1}}\int_{t_0}^{0}\frac{dt}{\sqrt{(1-t^2)(1-m^2t^2)}} \qquad (6)$$

is a constant which can be expressed in terms of the periods of $sn(x)$, and φ_0 is the initial value of φ.

We then get the function $r(\varphi)$:

$$r = \left(\frac{4(v_2 - v_1)}{sn^2\Big((\varphi - \varphi')\sqrt{v_2 - v_1}\Big)} + 4v_1 + \frac{1}{3}\right)^{-1} . \qquad (7)$$

A. Construction of the wormhole and embedding

To obtain the Schwarzschild thin-shell wormhole we follow the ‘surgery’-method of Visser [5, 6]. This method was also applied by Kashgarin and Sushkov [14] for the constuction of the Kerr thin-shell wormhole (see Sec. III A). The procedure is as follows: we cut the Schwarzschild spacetime outside the event horizon $h = 1$ at some value of the radial coordinate b_0, where b_0 is now the throat parameter and $b_0 > h$. Gluing two copies of the asymptotically flat region $r \geq b_0$, which are then connected by a wormhole with the throat hypersurface Σ, we obtain a geodesically complete manifold. The coordinate $|l| = |r - b_0|$ such that $l \in (-\infty, \infty)$ then covers the whole spacetime (the upper and the lower universe). The throat of the wormhole is located at $l = 0$.

To visualize the topology of the wormhole we consider a two-dimensional hypersurface ($t = const, \vartheta = \pi/2$) [25]. Embedded into the Euclidean space with the cylindrical coordinates (r, φ, z)

$$z(r) = 2\sqrt{r-1} - 2\sqrt{b_0 - 1} , \qquad (8)$$

this hypersurface leads to the embedding diagram visualized in Fig.2. (In the next section we discuss the orbits in the thin-shell Schwarzschild-wormhole spacetime and show an example for the embedding diagram of an orbit.)

B. Geodesics

We start with the effective potential defined by the expression [38]

$$V_{\text{eff}} = \left(\delta + \frac{L^2}{r^2}\right)\left(1 - \frac{1}{r}\right) . \qquad (9)$$

Figure 1 shows examples of the effective potential for massive test particles with $\delta = 1$ for different values of b_0. Here the coordinate l was used. The following types of orbits exist in the Schwarzschild-wormhole spacetime for massive test particles:

Type A two-world escape orbit TWE which connect two parts of the Universe. These orbits would be ending at the singularity in usual Schwarzschild spacetime.

Type B two-world bound orbits TWB when a test particle moves on a bound orbit stretching from one into another part of the Universe. This orbit connects the upper and lower parts of the universe similar to the orbit of type A.

Type C this type contains two possible orbits: two-world bound TWB and escape orbits EO. EOs exist in both parts of the Universe. For growing values of the throat parameter b_0 this type reduces to C_0 containing only EOs. See Fig.1(b).

Type D this type includes two-world bound TWB and bound orbits BO. BOs exist in both parts of the Universe. Here again D reduces to type D_0 for growing values of the throat parameter b_0. See Fig.1(b).

For large b_0-values only orbits of type B and A survive (Fig.1(c)). For very large values - only type A is possible.

Figure 1(d) shows a set of potential plots for large $L^2 = 9$, when no planetary bound orbits are possible (also in the Schwarzschild black hole spacetime), and different values of the throat parameter b_0.

Geodesics of massive test particles described by the solution (7) are shown in Fig.2. In this Figure, the two-world bound TWB orbit (a) and the bound orbit BO (b) correspond to type D. The two-world bound TWB orbit (c) and the escape orbit EO (d) are of type C, and the two-world-escape orbits TWE (e) and (f) are of type A. The orbits are embedded into the three-dimensional space with the coordinates (x, y, z), where $x = r\cos(\varphi)$, $y = r\sin(\varphi)$, and r and z are given by (7) and (8) correspondingly.

a. Geodesics for $\delta = 0$. Similar to the Schwarzschild black hole spacetime no planetary bound orbits exist in the Schwarzschild thin-shell wormhole spacetime. The orbits of type A (two-world escape TWE), B (two-world bound TWB) and C (two-world bound TWB and escape EO) are possible. We show some examples in Fig.3.

III. KERR WORMHOLE

Geodesic motion of a test particle in the equatorial plane is described by the equation [38]

$$\left(\frac{dr}{d\gamma}\right)^2 = E^2r^4 + r^2(a^2E^2 - L^2) - \delta\Delta r^2 + r(aE - L)^2 \quad (10)$$

$$\frac{d\varphi}{d\gamma} = \frac{r}{\Delta}\left(Lr + (aE - L)\right) , \quad (11)$$

where E and L are again dimensionless conserved energy and angular momentum, a is a dimensionless rotation parameter. $\Delta = r^2 + a^2 - r$, δ is zero for null geodesics and is one for time-like geodesic, γ is the proper time. The radial coordinate is again normalized to $2M$.

The ergosphere for the equatorial plane is located at $r = 1$. The vanishing of Δ defines the two horizons of the Kerr spacetime: $h_{1,2} = (1 \mp \sqrt{1 - 4a^2})/2$.

b. Radial equation. By the transformation $r = a_3(4y - a_2/3)^{-1}$, the equation (10) reduces to the Weierstrass form [42]

$$\left(\frac{dy}{d\gamma}\right)^2 = 4y^3 - \nu_2 y - \nu_3 = P_3(y) , \quad (12)$$

where $\nu_2 = (a_2^2/3 - a_1a_3)/4$ and $\nu_3 = a_1a_2a_3/48 - a_0a_3^2/16 - a_2^3/216$. The coefficients a_i read:

$$a_3 = (aE - L)^2,\ a_2 = a^2(E^2 - \delta) - L^2 ,$$
$$a_1 = \delta,\ a_0 = E^2 - \delta . \quad (13)$$

The solution of the differential equation (12) is the Weierstrass $\wp$-function $y = \wp(\gamma - \gamma')$, where $\gamma' = \gamma_0 + \int_{y_0}^{\infty}(4y^3 - \nu_2 y - \nu_3)^{-1/2}dy$ is a constant defined by the initial conditions of the geodesic. With this result, the final solution for the coordinate r yields:

$$r = \frac{3a_3}{12\wp(\gamma - \gamma') - a_2} . \quad (14)$$

c. Azimuthal equation. The transformation $r = a_3(4y - a_2/3)^{-1}$, reduces the equation (11) to a sum of two differentials of the third kind:

$$d\varphi = \sum_{i=1}^{2} \frac{K_i}{y - y_i}\frac{dy}{\sqrt{P_3(y)}} , \quad (15)$$

where the constants K_1 and K_2 are defined as

$$K_i = \frac{(-1)^{i-1}}{\sqrt{1 - 4a^2}}\frac{a_3}{4}\left(L + \frac{(aE - L)(2a^2)^{-1}}{\left(1 + (-1)^{i-1}\sqrt{1 - 4a^2}\right)^{-1}}\right) , \quad (16)$$

and $i = 1, 2$.

To proceed, we introduce $w = \gamma - \gamma'$ and replace y in (15) by $y = \wp(w)$. This yields

$$d\varphi = \sum_{i=1}^{2} \frac{K_i}{\wp(w) - \wp_{y_i}}dw , \quad (17)$$

where $\wp_{y_i}$, $i = 1, 2$, is defined by the equation $\wp_{y_i} = \wp(w_{y_i}) = y_i$.

The integration of (17) in terms of elliptic ζ and σ functions reads [42–45]

$$\varphi = \varphi_0 + \sum_{i=1}^{2} \frac{K_i}{\wp'(w_{y_i})}\left(2\zeta(w_{y_i})(w - w_0) + \ln\frac{\sigma(w - w_{y_i})}{\sigma(w + w_{y_i})} - \ln\frac{\sigma(w_0 - w_{y_i})}{\sigma(w_0 + w_{y_i})}\right) , \quad (18)$$

where $w_0 = w(\gamma_0)$.

A. Construction of the wormhole and embedding

The throat of the Kerr wormhole lies behind the horizons: $b_0 > h_2$. Following [14] we assume that the thin-shell Kerr-wormhole with the throat parameter b_0 does not depend on the proper time and, thus, is constant. Similar to the Sec. II A we use the surgery method to construct the thin-shell Kerr-wormhole. Namely, we cut the Kerr spacetime at some $b_0 > h_2$ and glue two copies of the manifold $M_{1,2} = (t, r, \vartheta, \varphi | r \geq b_0)$ onto each other. Identifying the boundaries of these copies we get a new geodesically complete manifold with two regions connected by a wormhole with the throat characterized by the parameter b_0. The new coordinate $|l| = |r - b_0|$ running from $-\infty$ to ∞ and vanishing at the throat is a practical coordinate to portray the effective potential (22) (see Fig.4 and Fig.5 in the Sec.III B).

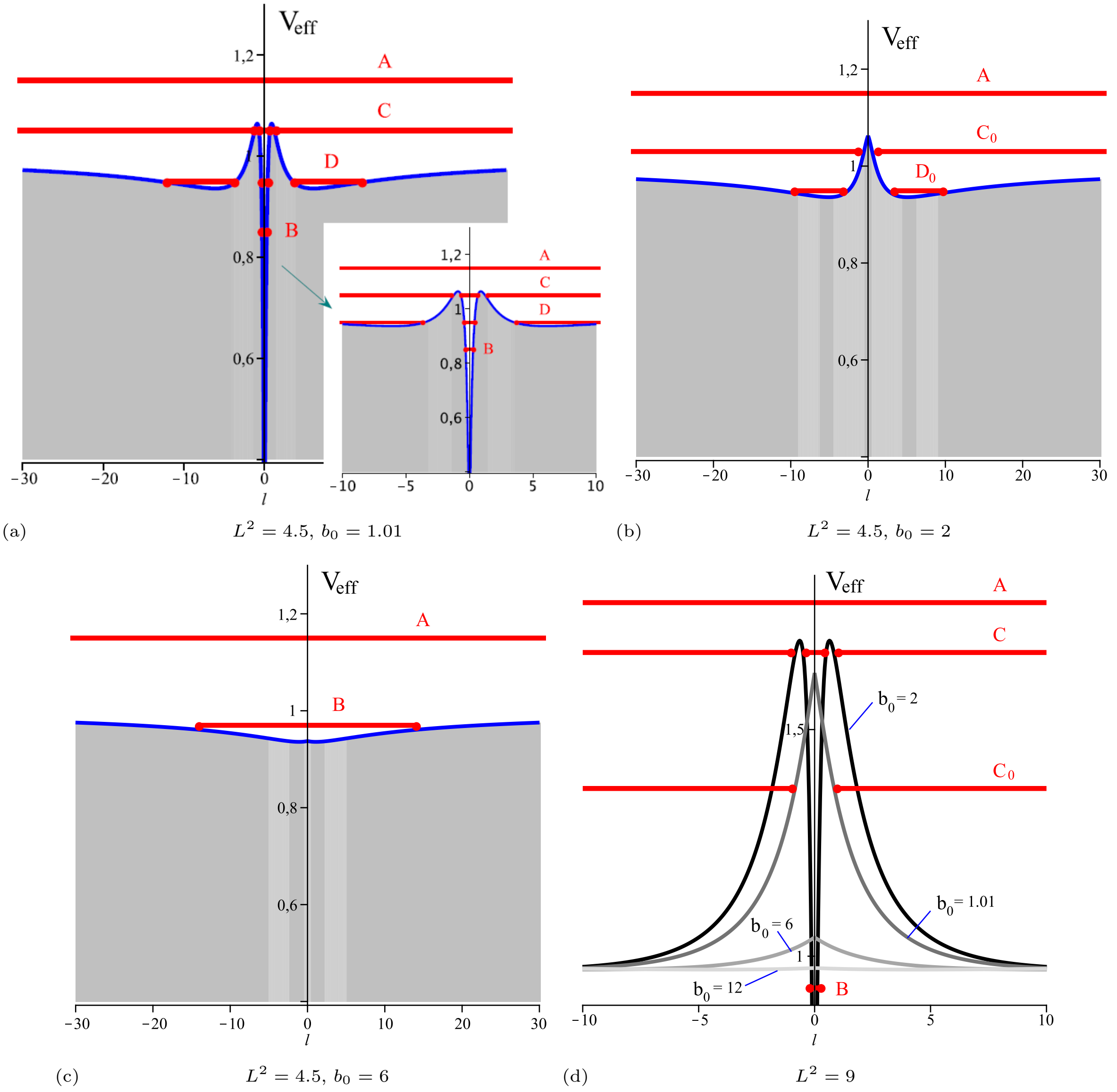

(a) $L^2 = 4.5,\ b_0 = 1.01$ (b) $L^2 = 4.5,\ b_0 = 2$

(c) $L^2 = 4.5,\ b_0 = 6$ (d) $L^2 = 9$

FIG. 1: The effective potential (eq. (9)) in the Schwarzschild wormhole spacetime for $\delta = 1$. Filled regions in (a)-(c) mean forbidden energy values. Only in (d) we did not color the forbidden regions in order not to overcharge the picture. For a growing throat of the wormhole no planetary bound orbits exist. The orbit of type A corresponds to the two-world escape orbit passing through the upper and lower parts of the Universe. The orbit of type B is a two-world bound orbit. The orbits of type D include planetary bound orbits, and orbits of type C include escape orbits in both parts of the Universe. For details see Sec. II B.

To understand the Kerr-wormhole topology for the equatorial plane motion described by the functions (14) and (18), consider the two dimensional hypersurface $(t = const, \vartheta = \pi/2)$ described by the geometry:

$$ds_0 = \frac{r^2}{\Delta}dr^2 + \left(r^2 + a^2 + \frac{a^2}{r}\right)d\varphi^2$$
$$= \frac{r^2}{\Delta}dr^2 + R^2 d\varphi^2 \ , \tag{19}$$

where $R^2 = r^2 + a^2 + \frac{a^2}{r}$ and $\Delta = r^2 + a^2 - r$. This two-dimensional hypersurface can be embedded into the Euclidean space given by

$$ds_E = dR^2 + R^2 d\varphi^2 + dz^2$$
$$= \left(\left(\frac{dR}{dr}\right)^2 + \left(\frac{dz}{dr}\right)^2\right)dr^2 + R^2 d\varphi^2 \tag{20}$$

in the cylindrical coordinates (r, φ, z).

Comparing the coefficients by dr^2 in (19) and (20) we find that the shape of the embedding diagram in the Euclidean space is given by the integral

$$z(r) = \int_{b_0}^{r} \sqrt{\frac{r'^2}{\Delta} - \frac{(2r'^3 - a^2)^2}{4r'^3(r'^3 + a^2(r'+1))}}dr' \tag{21}$$

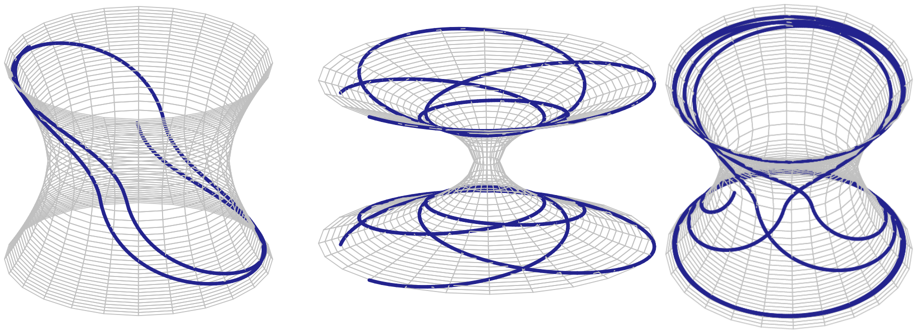

(a) $L^2 = 4.5, E^2 = 0.949$. TWB. (b) $L^2 = 4.5, E^2 = 0.949$. BO. (c) $L^2 = 7.3, E^2 = 1.451867$. TWB.

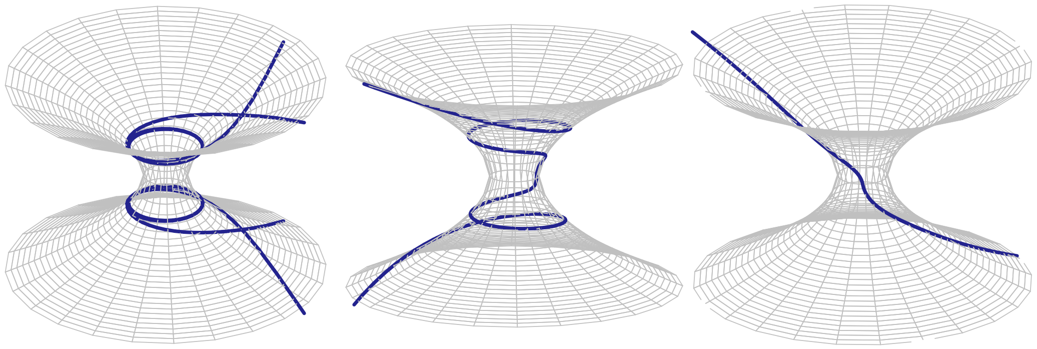

(d) $L^2 = 7.3, E^2 = 1.451867$. EO. (e) $L^2 = 4.3, E^2 = 1.04$. TWE. (f) $L^2 = 9, E^2 = 3$. TWE.

FIG. 2: Orbits of a test particle with $\delta = 1$ for different values of angular momentum and energy in the thin-shell Schwarzschild wormhole spacetime. The two-world-bound (TWB) and two-world-escape (TWE) orbits extend from the upper to the lower part of the Universe connected by a wormhole with throat parameter $b_0 = 1.01$.

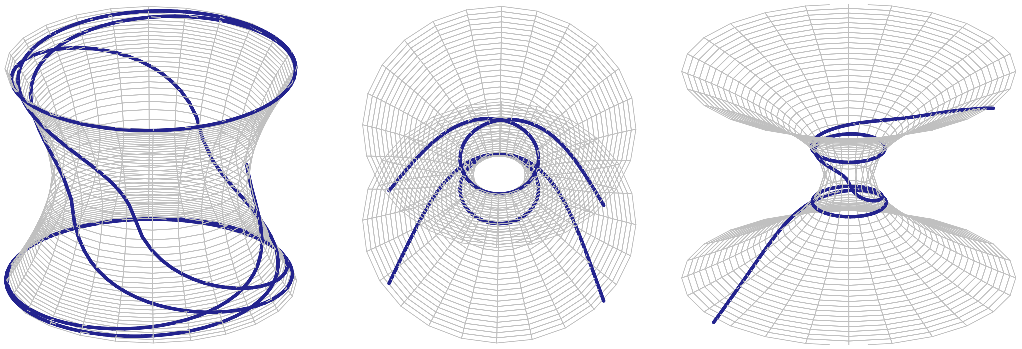

(a) $L^2 = 4.5, E^2 = 0.6665$. TWB. (b) $L^2 = 4.5, E^2 = 0.6665$. EO. (c) $L^2 = 4.5, E^2 = 0.6667$. TWE.

FIG. 3: Orbits in the thin-shell Schwarzschild wormhole spacetime for a massless test particle ($\delta = 0$). The two-world-bound (TWB) and two-world-escape (TWE) orbits are located in the upper and lower parts of the Universe which are connected by a wormhole with throat parameter $b_0 = 1.01$.

and is visualized in Fig.6 (to the discussion of the orbits we will come in the next section).

B. Geodesics

The effective potential in the Kerr spacetime reads [38, 41]

$$V_{\text{eff}} = \frac{aL \pm \sqrt{r\Delta\left(rL^2 + \delta\left(r^3 + a^2(r+1)\right)\right)}}{r^3 + a^2(r+1)} \,. \tag{22}$$

Its graphical representation is shown in Fig.4, where the coordinate $|l| = |r - b_0|$ is used.

The orbit types in the thin-shell Kerr-wormhole are very similar to those in the thin-shell Schwarzschild-wormhole. Namely,

Type A two-world escape orbit TWE which connects two regions of the Universe. In the Kerr black hole spacetime this orbit would continue into the negative radial coordinate region.

Type B two-world bound orbits TWB. A test particle moves on a bound orbit which is partly located in the lower (respectively, upper) Universe, so that, a particle flies through the throat.

Type C here two-world bound TWB and escape orbits EO are possible. EOs exist in both parts of the Universe. For growing values of the throat parameter b_0 this type reduces to C_0 containing only EOs. See Fig.4(c).

Type D two-world bound TWB and bound orbits BO are possible. BOs exist in both parts of the Universe. For growing values of the throat parameter b_0 the type D reduces to D_0 containing only BOs (see Fig.4(c)).

For a further growing throat parameter b_0, TWB (type B) and TWE (type A) exist (see Fig.4(d)). For larger b_0 only the TWE (type A) orbits remain. In Fig.5 we make L (in (a)) and a (in (b)) change. In the first case, similar to the Kerr black hole spacetime, for large angular momenta of a test particle no planetary bound orbits exist. In the second case the form of the effective potential transforms when a tends to the critical value $a_{\text{crit}} = 0.5$ when the horizons in the Kerr black-hole spacetime merge.

We illustrate these orbit types in Figs.6 and 7. Fig. 7, plotted for opposite signs of the rotation parameter of the wormhole and the angular momentum of a test particle, also shows the influence of the ergosphere. It can be recognized in the directional change taking place shortly before the black circle is approached, which symbolizes the wormhole throat in the pictures (a) for the TWB and (d) for the TWE orbit. The ergoregion in the Kerr wormhole spacetime surrounds the throat. The corresponding embedded orbits are shown in (b) and (e).

d. Geodesics for $\delta = 0$. Like in the Kerr black hole spacetime no planetary bound orbits exist in the Kerr thin-shell wormhole spacetime, and only the orbits of type A (two-world escape TWE), B (two-world bound TWB) and C (two-world bound TWB and escape EO) can be found. Fig.8 visualizes some orbits for corotating massless test particles and Fig.9 for counterrotating ones. In the last case a particle is dragged into the direction of wormhole rotation in the vicinity of ergosphere which is best seen in the projections 9(a) for the embedded two-world bound orbit (b) and 9(d) for the embedded two-world escape orbit (e).

IV. CONCLUSION

We have studied the motion of massive and massless test particles in the Schwarzschild and Kerr thin-shell wormhole spacetimes. These traversable wormhole spacetimes were constructed by the cut-and-paste method and represent geodesically complete manifolds. The solution of the geodesic equations is given analytically in terms of elliptic Jacobi and Weierstrass functions. Planetary bound orbits exist only for not too wide a throat of the wormhole in both cases. If the throat is sufficiently narrow (i.e. the throat parameter is chosen to be smaller than the ergosphere), a test particle is dragged into the direction of the wormhole rotation in the vicinity of the ergosphere. Here extraction of energy due to the Penrose process is possible.

ACKNOWLEDGEMENT

We would like to thank Jutta Kunz and Burkhard Kleihaus for helpful discussions. We also gratefully acknowledge financial support of the German Research Foundation DFG and the support within the framework of the DFG Research Training Group 1620 *Models of gravity*.

[1] A. Einstein, N. Rosen, *Phys. Rev.* **48**, 73 (1935)
[2] J. A. Wheeler, *Geometrodynamics* (Academic Press, New York, 1962)
[3] R. W. Fuller, J. A. Wheeler, *Phys. Rev.* **128**, 919 (1962)
[4] M. S. Morris, K. S. Thorne, *Wormholes in spacetime and their use for interstellar travel: a tool for teaching general relativity*, *Am. j. Phys.* **56**, 395 (1988)
[5] M. Visser, *Traversable wormholes: some simple exmaples*, *Phys. Rev. D* **39**, 3182 (1989)
[6] M. Visser, *Traversable wormholes from surgically modified Schwarzschild spacetimes*, *Nuclear Physics B* **328**, 203 (1989)
[7] S. Shushkov, *Wormholes supported by a phantom energy*, *Phys. Rev. D* **71**,043520 (2005)
[8] F. S. N. Lobo, *Phantom energy traversable wormholes*, *Phys. Rev. D* **71**,084011 (2005)
[9] O. B. Zaslavskii, *Exactly Solvable Model of a Wormhole Supported by Phantom Energy*, *Phys. Rev. D*, **72**, 061303 (2005)
[10] P. K. F. Kuhfittig, *Seeking Exactly Solvable Models of Traversable Wormholes Supported by Phantom Energy*, *Class. Quantum Grav.*, **23**, 5853 (2006)

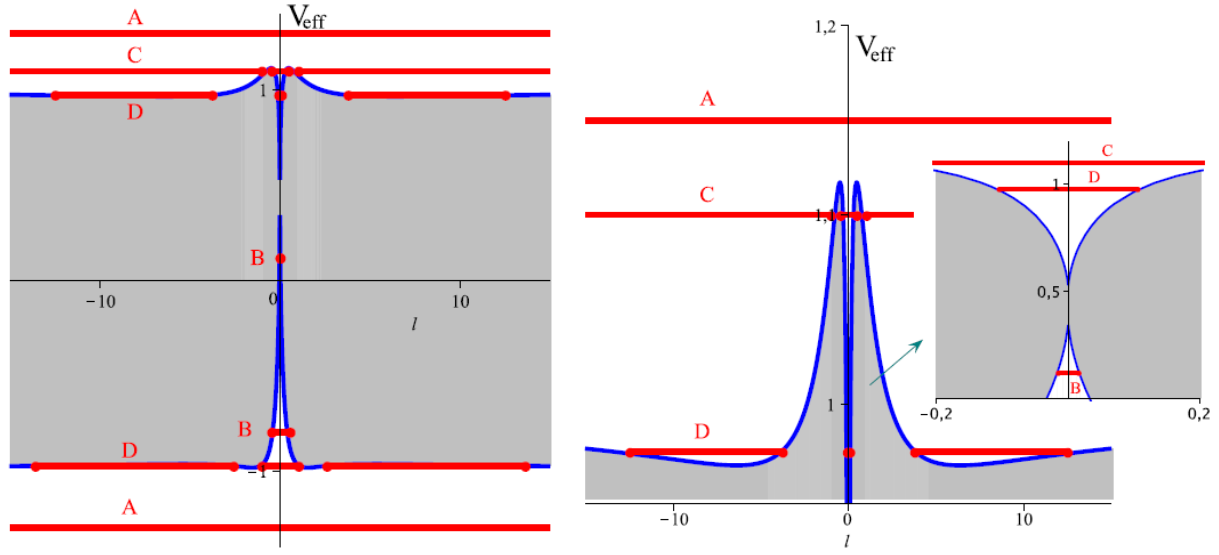

(a) $b_0 = 0.96$ (b) Detailed representation of the potential (a).

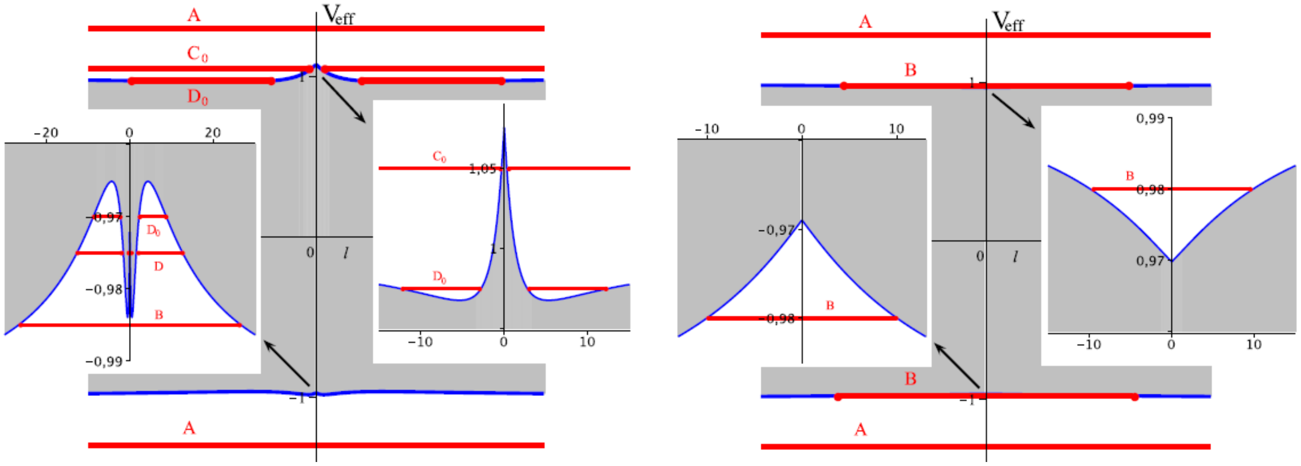

(c) $b_0 = 2.0$ (d) $b_0 = 10.0$

FIG. 4: The effective potential (eq. (22)) for $\delta = 1$ and $L = 2.1$. $a = 0.2$ in the Kerr wormhole spacetime. $b_0 > h_2$. Filled grey regions denote forbidden energy values. See Sec.III B for details.

[11] F. Rahaman, M. Kalam, M. Sarkar, K. Gayen, *A Theoretical Construction of Wormhole Supported by Phantom Energy*, Phys. Lett. B, **633**, 161 (2006)
[12] A. Das, S. Kar, *The Ellis wormhole with 'tachyon matter'*, *Class. Quantum Grav.* **22**, 3045 (2005)
[13] F. S. N. Lobo, *Chaplygin traversable wormholes*, *Phys. Rev. D* **73**, 064028 (2006)
[14] P. E. Kashgarin, S. V. Sushkov, *Rotating Thin-Shell Wormhole from Glued Kerr Spacetimes*, *Gravitationa and Cosmology* **17**, 119 (2011)
[15] P. K. F. Kuhfittig, *Can a wormhole supported by only small amounts of exotic matter really be traversable?*, *Phys. Rev. D*, **68**, 067502 (2003)
[16] P. K. F. Kuhfittig, *Wormholes supported by a combination of normal and quintessential matter in Einstein and Einstein-Maxwell gravity*, arXiv:1212.0153 [gr-qc]
[17] M. Visser, *Wormholes: from Einstein to Hawking* (American Institute of physics, Woodbury, 1995)
[18] F. S. N. Lobo, *Exotic solutions in General Relativity: Traversable wormholes and "warp drive" spacetimes*, arXiv:0710.4474, to appear in an edited collection 'Classical and Quantum Gravity Research Progress', Nova Science Publishers
[19] F. Rahaman, P.K.F. Kuhfittig, S. Ray, S. Islam, *Searching for higher-dimensional wormholes with noncommutative geometry*, *Phys. Rev. D* **86**, 106010 (2012)
[20] P.K.F. Kuhfittig, *On the Stability of Thin-Shell Wormholes in Noncommutative Geometry*, *Advances in High Energy Physics*, **2012** Article ID 462493 (2012)
[21] P. Kanti, B. Kleihaus, J. Kunz, *Wormholes in Dilatonic Einstein-Gauss-Bonnet Theory*, *Phys. Rev. Lett.* **107**, 271101 (2011)
[22] P. Kanti, B. Kleihaus, J. Kunz, *Stable Lorentzian wormholes in dilatonic Einstein-Gauss-Bonnet theory*, *Phys. Rev. D* **85**, 044007 (2012)

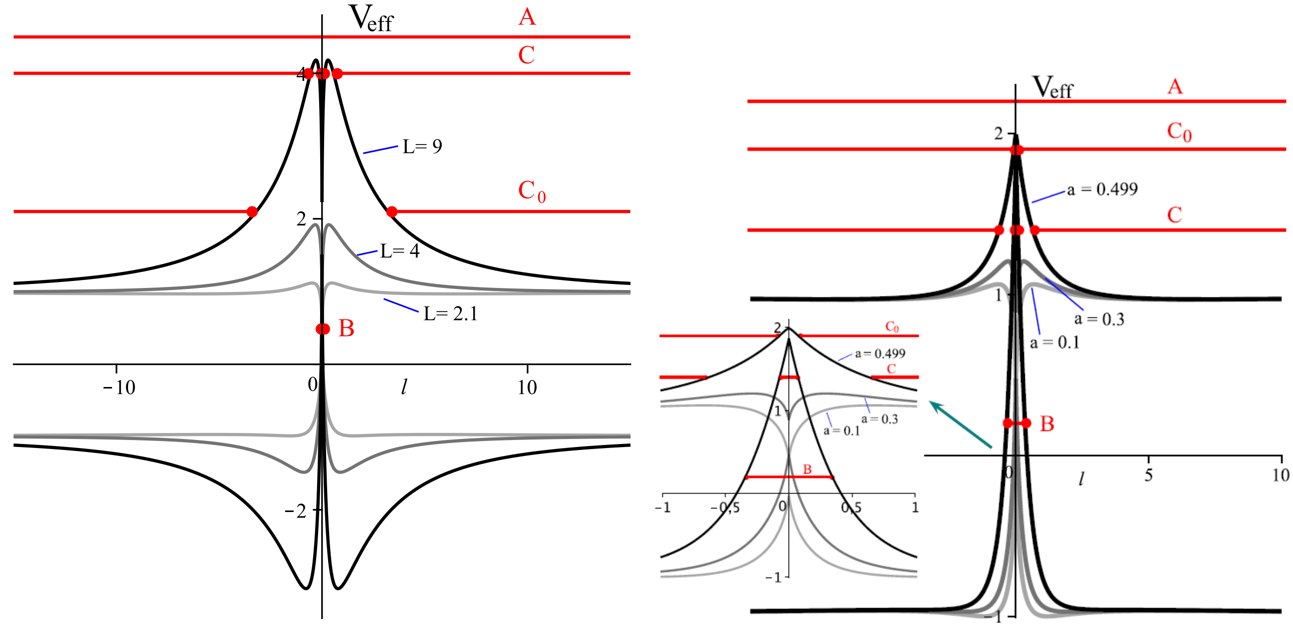

(a) $a = 0.2,\ b_0 = 0.96$

(b) $L = 2.1,\ b_0 = h_2 + 0.01$

FIG. 5: The effective potential (eq. (22)) for $\delta = 1$ and different values of L (a) and a (b) in the thin-shell Kerr wormhole spacetime. $b_0 > h_2$. When keeping a constant and increasing L in (a), we see that planetary bound orbits (i.e. of type D) do not exist (as expected from the Kerr black hole spacetime). When keeping L constant and increasing a in (b), we observe the form of the effective potential change. We show the possible orbit types (for positive energies) for the potential in black for an almost critical rotation parameter $a = 0.499$ and the value b_0 a bit larger than the horizon. In order not to overcharge the picture, we do not fill the forbidden regions with color (cp. Fig.4).

[23] V. Dzhunushaliev, V. Folomeev, B. Kleihaus, J. Kunz, *A star harbouring a wormhole at its core*, *JCAP* **04**, 031 (2011); DOI: 10.1088/1475-7516/2011/04/031

[24] V. Dzhunushaliev, V. Folomeev, B. Kleihaus, J. Kunz, *Mixed neutron-star-plus-wormhole systems: Equilibrium configurations*, *Phys. Rev. D* **85**, 124028 (2012)

[25] T. Müller, *Exact geometric optics in a Morris-Thorne wormhole spacetime*, *Phys. Rev. D* **77**, 044043 (2008)

[26] O. Sarbach, T. Zannias, *The propagation of particles and fields in wormhole geometries*, *AIP Conf.Proc.* **1473** 223 (2012); arXiv:1204.3977 [gr-qc]

[27] E. Teo, *Rotating traversable wormholes*, *Phys. Rev. D* **58**, 024014 (1998)

[28] P. K. F. Kuhfittig, *Axially symmetric rotating traversable wormholes*, *Phys. Rev. D* **67** 064015 (2003)

[29] P. E. Kashargin, S.V. Sushkov, *Slowly rotating scalar field wormholes: The second order approximation*, *Phys. Rev. D* **78**, 064071 (2008)

[30] T. Matos, D. Núñez, *Rotating scalar field wormhole*, *Class. Quantum Grav.* **23**, 4485 (2006)

[31] M. Jamil, *Can a wormhole generate electromagnetic field?*, *Int. J. Theor. Phys.* **49**, 1549 (2010)

[32] T. Matos, *Class of Einstein–Maxwell phantom fields: rotating and magnetized wormholes*, *Gen. Relativ. Gravit.*, DOI 10.1007/s10714-010-0976-6 (2010)

[33] M. S. Morris, K. S. Thorne, U. Yurtsever, *Wormholes, Time Machines, and the Weak Energy Condition*, *Phys. Rev. Lett.* **61**, 1446 (1988)

[34] V. P. Frolov, I. D. Novikov, *Physical effects in wormholes and time machines*, *Phys. Rev. D* **42**, 1057 (1990)

[35] V. P. Frolov, *Vacuum polarization in a locally static multiply connected spacetime and a time-machine problem*, *Phys. Rev. D* **43**, 3878 (1991)

[36] S. W. Kim, K. S. Thorne, *Do vacuum Fluctuations prevent the creation of closed timelike curves?*, *Phys. Rev. D* **43**, 3929 (1991)

[37] S. W. Hawking, *Chronology protection conjecture*, *Phys. Rev. D* **46**, 603 (1992)

[38] S. Chandrasekhar, *The Mathematical Theory of Black Holes* (Oxford University Press, Oxford, 1983).

[39] J. B. Hartle, *Gravity*, (Addison Wesley, San Francisco, 2003).

[40] B. F. Schutz, *A first course in general relativity*, (Cambridge University Press, Cambridge, UK, 1985).

[41] B. O'Neil, *The Geometry of Kerr Black Holes* (A.K. Peters, Wellesley, MA, 1995).

[42] A. I. Markushevich, *Theory of functions of a complex variable*, Vol. III, Prentice-Hall, Inc., Englewood Cliffs, N.J. (1967).

[43] S. Grunau, V. Kagramanova, *Geodesics of electrically and magnetically charged test particles in the Reissner-Nordström spacetime: analytical solutions*, *Phys. Rev. D* **83**, 044009 (2011).

[44] V. Kagramanova, S. Reimers, *Analytic treatment of geodesics in five-dimensional Myers-Perry spacetimes*, *Phys. Rev. D* **86**, 084029 (2012)

[45] V. Kagramanova, J. Kunz, E. Hackmann and C. Lämmerzahl, *Analytic treatment of complete and incomplete geodesics in Taub-NUT spacetimes*, Phys. Rev. D **81**, 124044 (2010)

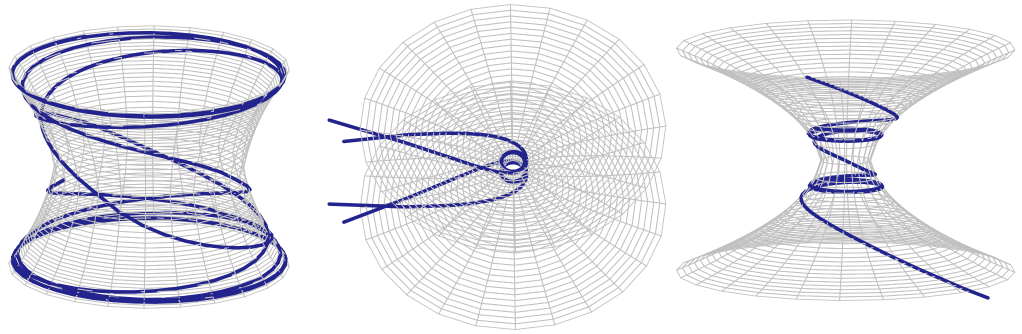

(a) $E = 1.11722, L = 2.1$. TWB. (b) $E = 1.11722, L = 2.1$. EO. (c) $E = 1.11723, L = 2.1$. TWE.

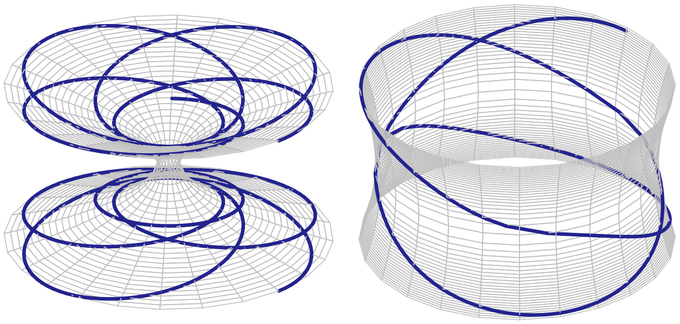

(d) $E = 0.975, L = 2.1$. BO. (e) $E = 0.975, L = 2.1$. TWB.

FIG. 6: Orbits for a test particle with $\delta = 1$ for different values of angular momentum and energy in the thin-shell Kerr wormhole spacetime. The two-world-bound (TWB) and two-world-escape (TWE) orbits stretch across the two regions of a Universe connected by a wormhole with throat parameter $b_0 = 0.99$ in ((a)-(c)) and $b_0 = 0.96$ in ((d)-(e)). Kerr–paramerer $a = 0.2$.

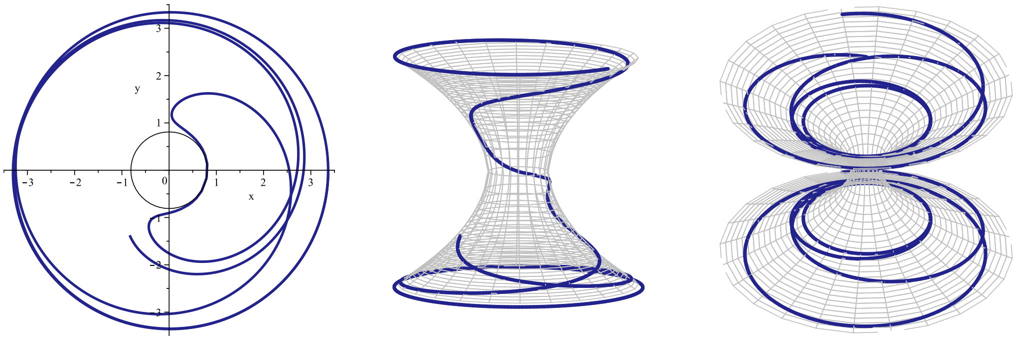

(a) $E = 0.96492, L = -2.1$. TWB. (b) $E = 0.96492, L = -2.1$. TWB. (c) $E = 0.96492, L = -2.1$. EO.

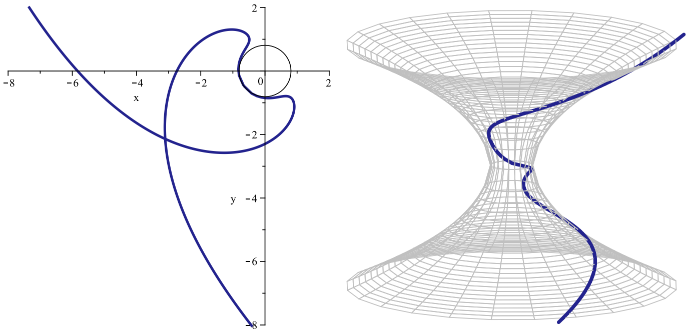

(d) $E = 1.01, L = -2.1$. TWE. (e) $E = 1.01, L = -2.1$. TWE.

FIG. 7: Orbits for a test particle with $\delta = 1$ for different values of angular momentum and energy in the thin-shell Kerr wormhole spacetime. Kerr–paramerer $a = 0.4$. The orbit (a) is the x-y projection of the orbit (b). The black circle is the throat $b_0 = 0.81$. A test particle with the negative value of the angular momentum is dragged in the direction of the Kerr-wormhole rotation. This happens in the vicinity of the ergoregion which surrounds the throat of the wormhole. The third orbit (c) is a bound orbit for the same E- and L-values. The described dragging can be also seen in the orbit shown in (e) and its x-y projection (d).

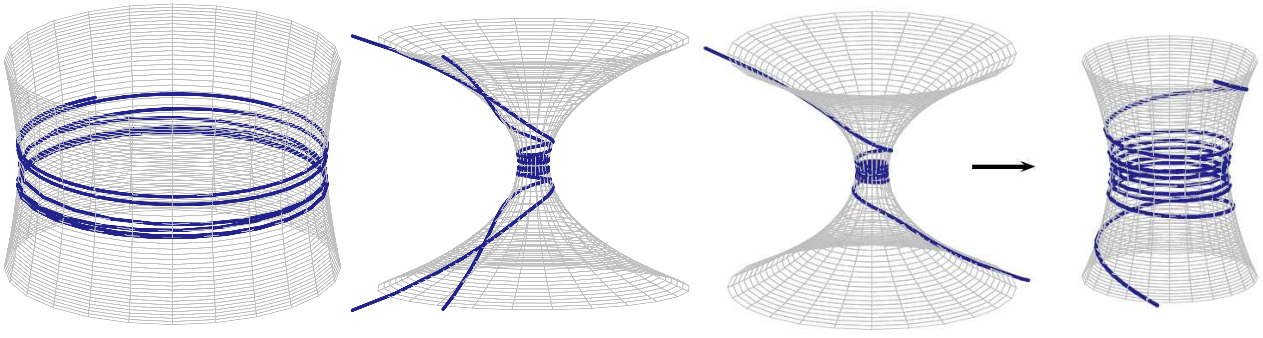

(a) $E = 1.271, L = 1.5$. TWB. (b) $E = 1.271, L = 1.5$. EO. (c) $E = 1.272, L = 1.5$. TWE.

FIG. 8: Orbits for a massless test particle ($\delta = 0$) in the thin-shell Kerr wormhole spacetime. Kerr–paramerer $a = 0.49$. Plot(a) shows a two-world bound orbit and plot(b) two escape orbits in the upper and lower parts of the Universe. Plot(c) shows a test particle moving in the upper and lower parts of the Universe on a two-world escape orbit. Here $b_0 = 0.61$.

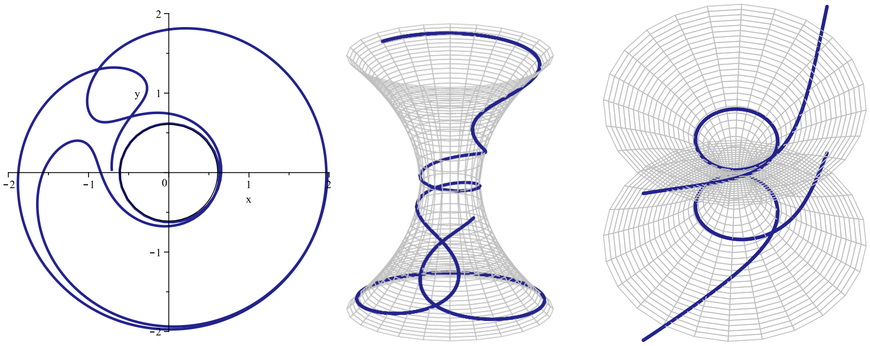

(a) $E = 0.4306, L = -1.5$. TWB. (b) $E = 0.4306, L = -1.5$. TWB. (c) $E = 0.4306, L = -1.5$. EO.

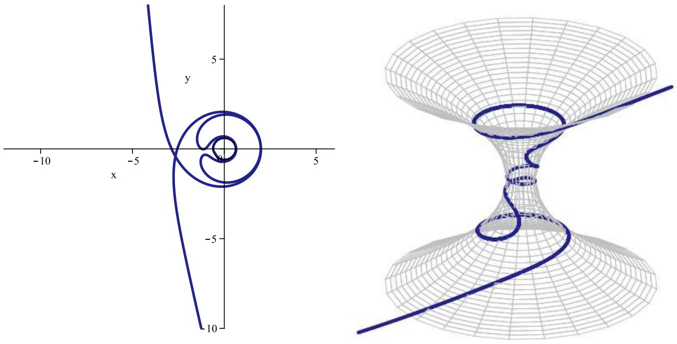

(d) $E = 0.4307, L = -1.5$. TWE. (e) $E = 0.4307, L = -1.5$. TWE.

FIG. 9: Orbits in the thin-shell Kerr wormhole spacetime for a massless test particle ($\delta = 0$) when a particle and a wormhole are counterrotating. Kerr–parameter $a = 0.49$. Plot(b) shows a two-world bound orbit and plot(c) two escape orbits in the upper and lower parts of the Universe. The picture(a) is a projection of (b) onto the x-y plane. Plots(d) and (e) show a two-world escape orbit extending over upper and lower parts of the Universe. Here $b_0 = 0.609$.